

# Four-Dimensional Constellations for Dual-Polarized Satellite Communications

Nicolò Mazzali, Farbod Kayhan, and Bhavani Shankar Mysore R

Interdisciplinary Centre for Security, Reliability and Trust (SnT), University of Luxembourg

(e-mails: {nicolo.mazzali, farbod.kayhan, bhavani.shankar}@uni.lu)

**Abstract**—In this paper, we investigate the performance of constellations optimized for transmissions in dual-polar mobile satellite applications. These four-dimensional constellations (in-phase and quadrature per polarization) are designed for joint transmission over the two polarizations. Such constellations enhance the reliability of the system by providing certain redundancy into their design. Their performance is compared with transmission of independent 2D constellations over each polarization. As performance metrics, the pragmatic achievable mutual information and the bit error rate have been considered. The gains serve to indicate the need to further investigate 4D constellation design and its application in dual-polar MIMO systems.

**Index Terms**—constellation design; pragmatic achievable mutual information; dual-polar MIMO; land-mobile satellite channel

## I. INTRODUCTION

In recent years, the continuously increasing demand of reliable communications at higher data rates has driven the scientific research towards spectrally efficient communication schemes that try to take full advantage of the available degrees of freedom. In this perspective, much effort has been dedicated to investigate many different diversity techniques, leading, for example, to space-time codes (STC) [1] and massive multiple-input multiple-output (MIMO) systems [2]. In satellite scenarios, time diversity may be an unpractical solution for applications with time constraints, while the spatial diversity required by MIMO systems sometimes cannot be provided by the satellite link [3]. On the other hand, polarization diversity has been regarded as an effective replacement for spatial diversity in satellite applications, where the number of antennas and their sizes are limiting features of the satellite transponder and the user terminal [3]. Several works have considered exploiting dual polarization in the S-band, e.g., [4] and [5]. The transmit processing in these works is performed after the modulation, while independent and joint decoding of streams have been considered. Moreover, these works are agnostic to the underlying constellation.

On the other hand, constellation design has been considered in terrestrial MIMO literature. Focussing on noncoherent reception where the receiver has no channel state information (CSI), finite cardinality constellations have been obtained in [6] by optimizing the cut-off rate, and the resulting constellations are actually a set of space-time codewords. For additional results on constellation design in noncoherent MIMO systems, the reader is referred to [7], [8], and references

therein. Constellation design with imperfect channel estimates at the receiver is considered in [9] and [10] among others. In most of the works on constellation design for MIMO systems, the adopted figure of merit for the optimization is the pairwise error probability and the union bound [11], [12]. Furthermore, the designed constellations are obtained by using standard constellations [13] or lattices [14]. Multidimensional constellation design has been a popular topic in the past, especially concerning the asymptotic performance when the number of dimensions grows large [15]. A thorough analysis of the trade-off among shaping gain, peak-to-average power ratio, and constellation-expansion ratio for an arbitrary number of dimensions can be found in [16].

In the paper, we focus on assessing the performance of constellations for dual-polar satellite systems serving mobile users. Contrary to the aforementioned approach, we assume no CSI at the transmitter and perfect CSI at the receiver. Since the transmitter does not have CSI, it assumes an additive white Gaussian noise (AWGN) channel for the design of four-dimensional (4D) constellations [17], where the number of dimensions is given by the number of components (in-phase and quadrature) used over the two polarizations. Moreover, since the receiver has full CSI, a joint processing of the two streams is considered. Such a setting can be construed as the traditional dual-polar MIMO, with constellation design implying transmit processing. Further, unlike the cited works on constellation design in MIMO systems, in this paper the main figure of merit is the pragmatic achievable mutual information (PAMI), as done in [18]. Such a choice allows for a joint optimization of the symbols and their labels, which is of paramount importance for multidimensional constellations of practical use [17]. Indeed, most of the recent works on multidimensional constellations assess the performance in terms of symbol error rate or in uncoded systems [19], neglecting the design of a suitable labelling for the constellations. Moreover, the gain promised in uncoded systems usually disappears in coded systems, becoming sometimes a loss because of the unsuitability of classical mappings [17].

In the following, we assess the performance of 4D constellations obtained in three different ways: as Cartesian product of standard 2D constellations (which is equivalent to transmitting independently over the two polarizations or performing spatial multiplexing [3]), as Cartesian product of numerically optimized 2D constellations (as in [18]), and by means of an optimization performed directly in 4D (as in [17]). For all the

considered constellations, we investigate the performance over different channels commonly used in satellite communications. In [17], only AWGN was considered with focus on spectral efficiency, while this paper explores the idea of using the constellations to enhance reliability and the system robustness against fading. Numerical results are obtained for a variety of channels, and interesting parallels with dual-polar MIMO systems are eventually drawn. The results of this work indicate that gains can be obtained in dual-polar MIMO satellite systems by considering constellation design as being integral towards exploiting polarization diversity.

In this paper we adopt the following notation: normal lower-case symbols for scalars, bold lower-case symbols for vectors, bold upper-case symbols for matrices, and we denote with  $\cdot^T$  the transpose operator.

## II. SCENARIOS, MODELS, AND FIGURE OF MERIT

### A. Considered Scenarios

We consider a generic dual-polarized broadband satellite scenario that can be seen as an abstraction of many different practical satellite applications (e.g., Inmarsat S-band mobile services, as well as Fleet and Iridium Pilot for maritime applications). Such an abstract scenario can be specialized to a particular application simply by choosing an appropriate channel model. For example, mobile satellite services (MSS) in the L- and S-bands require the channel described in [20] and [21], whereas in the Ka-band the channel model can be the one proposed in [22] and [23]. Without loss of generality, we assume the polarizations to be circular, and left-hand (LH) or right-hand (RH) oriented.

### B. System Model

The considered system model is depicted in Fig. 1. The information bits  $\{b_n\}$  are encoded by a channel encoder and then mapped into the information symbols  $\{x_k\}$  belonging to a finite  $N$ -dimensional constellation  $\chi$ . In the following we consider only constellations with  $M = 2^m$  elements, which are referred to as constellation points or transmitted symbols. The transmitted symbols are associated to the bits at the input of the modulator through the one-to-one labelling  $\mu: \chi \rightarrow \{0, 1\}^m$ . For any given symbol  $x_k$ , we denote by  $\mu^i(x_k)$  the value of the  $i$ -th bit of the label mapped to it. Since our aim is to use both polarizations jointly, we consider symbols belonging to constellations with  $N = 4$  dimensions (one real and one imaginary component per polarization). Nevertheless, the transmission on the physical channel has to be done separately for each polarization. Therefore, a projection of the selected 4D symbol  $x_k$  onto two orthogonal 2D planes needs to be performed. The result of such a projection are the 2D projected symbols  $x_{k,RH}$  and  $x_{k,LH}$  which are to be transmitted on the RH and LH circular polarizations, respectively. The projection operation is peculiar of dual-polar systems using non-Cartesian-based 4D constellations. Indeed, systems using Cartesian-based 4D constellations are equivalent in principle to dual-polar MIMO systems with spatial multiplexing, which do not require any projection because the projected 2D constellations would be

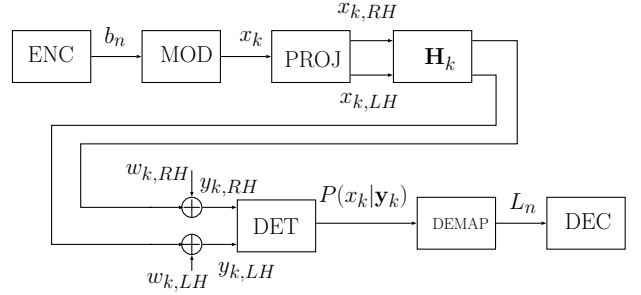


Fig. 1. System model.

identical to the 2D constellations chosen for the construction of the 4D constellation, as explained in Section III.

In the following, we assume the information symbols  $\{x_k\}$  to be independent and uniformly distributed random variables. It is worth noting that, depending on the chosen 4D constellation  $\chi$ , the projected symbols  $x_{k,RH}$  and  $x_{k,LH}$  may have a non-uniform probability distribution (see, for example, [17] and [19]) and may be correlated [16]. We denote by  $\mathbf{x}_k = [x_{k,RH}, x_{k,LH}]^T$  the vector containing the 2D projected symbols transmitted on the two polarizations at time  $k$ .

The channel is modeled by the  $2 \times 2$  matrix  $\mathbf{H}_k$  and the distribution of its entries depends on the considered scenario. The discrete-time received signal can be written therefore as

$$\mathbf{y}_k = \mathbf{H}_k \mathbf{x}_k + \mathbf{w}_k$$

where  $\mathbf{y}_k = [y_{k,RH}, y_{k,LH}]^T$  denotes the received symbols, and  $\mathbf{w}_k = [w_{k,RH}, w_{k,LH}]^T$  the samples of the AWGN process introduced by the channel. On each polarization, we assume the additive noise component  $w_{k,q}$  to be a circularly-symmetric complex Gaussian random variable with mean zero and variance  $\sigma_n^2$  per component, where  $q$  identifies the two polarizations. Moreover, we consider symbols, AWGN, and fading realizations to be mutually independent.

The possible correlation between  $x_{k,RH}$  and  $x_{k,LH}$  causes a performance loss if the detection is undertaken separately on each polarization. Therefore, only joint detection over the polarizations will be considered in the following. The chosen detection strategy is the soft maximum likelihood, providing as output of the detector, at every time  $k$ , the set of  $M$  a posteriori probabilities  $\{P(x_k|\mathbf{y}_k)\}$  [24]. These probabilities are then converted into log-likelihood ratios  $L_n$  by the demapper and passed to the soft decoder for the final decoding process. Finally, perfect CSI is assumed to be available at the receiver but not at the transmitter.

### C. Channel Models

For the ease of notation, we consider the generic time-varying fading channel denoted in Fig. 1 by

$$\mathbf{H}_k = \begin{bmatrix} h_{k,RR} & h_{k,LR} \\ h_{k,RL} & h_{k,LL} \end{bmatrix} \quad (1)$$

where the distribution of the entries depends on the chosen channel under investigation. Namely, the performance assessment is done over fading and land-mobile satellite (LMS) channels. So as to assess the performance in a variety of

fading conditions, a Rice channel has been used for excellent and medium line-of-sight (LOS) signal power, while the Rayleigh channel has been adopted for the totally non-line-of-sight (NLOS) condition [24]. For the Ricean fading, we use the model described in [5], which also includes cross-polar discrimination (XPD) and mobility effects. As an ideal case, we consider Rayleigh flat fading without cross-polar effects [24]. On the other hand, the LMS channel is a common assumption for mobile satellite applications and is characterized by Rayleigh-distributed multipath and lognormally distributed shadowing [20]. In particular, we employ the channel model detailed in [21], which describes the time variations of the channel by means of a two-state Markov chain. Moreover, it also includes: (i) shadowing effects (by resorting to the Loo distribution [25]), (ii) XPD effects stemming from the environment and the antenna characteristics, (iii) polarization correlation for large scale fading (which is lognormally distributed) and for the small scale fading (which is Rayleigh distributed), as well as (iv) temporal correlation induced by mobility [21]. For further details on the Rice and the LMS channels, the reader is referred to [5] and [21], respectively, and references therein.

#### D. Pragmatic Achievable Mutual Information

It is well known that the performance of a system is sensitive to the labelling when detection and decoding are performed separately [26]. Therefore, a careful constellation design needs to take the labelling into account, leading to a joint optimization of the constellation symbols and the corresponding labels. Thus, we choose the PAMI as objective function of the optimization procedure (as well as performance metric along with the bit error rate). Indeed, for a given constellation  $\chi$  and the corresponding labelling  $\mu$ , the PAMI in [26] is defined as

$$I_p(\chi, \mu) = \sum_{i=1}^m I(\mu^i(x); y) \quad (2)$$

where  $I(\cdot; \cdot)$  is the mutual information function and  $\mu^i(x)$  is the random variable indicating the  $i$ -th bit associated to the transmitted symbol. For the fading channels with perfect CSI at the receiver, Eq. (2) can be written as

$$I_p(\chi, \mu) = \frac{1}{M} \sum_{i=1}^m \sum_{x \in \chi} E_{w,h} \left\{ \log \frac{P(y|\mu^i(x))}{P(y)} \right\} \quad (3)$$

where the expectation is taken with respect to both the AWGN and the fading distributions. Since in most cases a closed-form expression for the expectation in (3) is not known, numerical methods are usually adopted to evaluate (3).

### III. 4D CONSTELLATION DESIGNS

The simplest way to obtain a  $M$ -ary 4D constellation is by taking the Cartesian product of two 2D constellations (e.g.,  $\sqrt{M}$ -QAM or  $\sqrt{M}$ -PSK standard constellations), called constituent constellations [16]. Since the projection onto a 2D plane can be viewed as the inverse of the Cartesian product, in

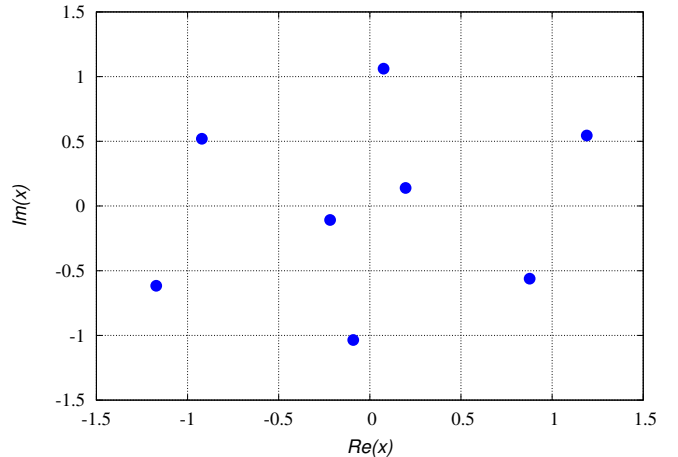


Fig. 2. Optimized 2D 8-ary constellation.

this case the two 2D projected constellations simply become the constituent 2D constellations. On the contrary, if the 4D constellation is not obtained as Cartesian product of two 2D constellations, then the projection onto a 2D plane may induce a shaping in the projected 2D constellation [17]. The possible shaping generated by the 2D projection introduces a correlation between the projected symbols  $x_{k,RH}$  and  $x_{k,LH}$ , which is independent of the correlation introduced by the channel.

In the following, we consider 64-ary constellations in order to exploit the constellations provided in [17]. Optimized constellations with a lower cardinality (i.e., 16-ary constellations) show, over the AWGN channel, a negligible gain over  $\sqrt{M} \times \sqrt{M}$ -QAM that does not justify further investigations [17]. On the other hand, higher order constellations are left for future works. Our benchmark constellations are constructed by taking the Cartesian product of two 8-QAM or two 8-PSK constellations. This means that each of the eight symbols belonging to a projected 2D constellation (8-QAM or 8-PSK) can be associated to any other symbol belonging to an identical constellation on the other polarization to form a 4D symbol (i.e., the 2D projected constellations are independent). These constellations are equivalent to the traditional spatial multiplexing in dual-polar MIMO [3]. We denote the resulting 4D constellations respectively by  $8 \times 8$ -QAM and  $8 \times 8$ -PSK.

However, the performance of Cartesian-based constellations can be improved by an accurate design of the constituting 2D constellation [17]. To this purpose, we choose the optimized 2D constellation presented in [17]. This constellation maximizes the PAMI over the AWGN channel at a signal-to-noise ratio equal to 10 dB with an average power constraint. Since the transmitter has no CSI, cross-polar effects have not been taken into account in order to make the optimized constellation independent of the environment. The shape of this 2D constellation is shown in Fig. 2 and the resulting 4D constellation, obtained by means of the Cartesian product, is denoted by  $8 \times 8$ -OPT.

Further improvement of the performance can be achieved by a joint optimization over the four dimensions. The coordinates

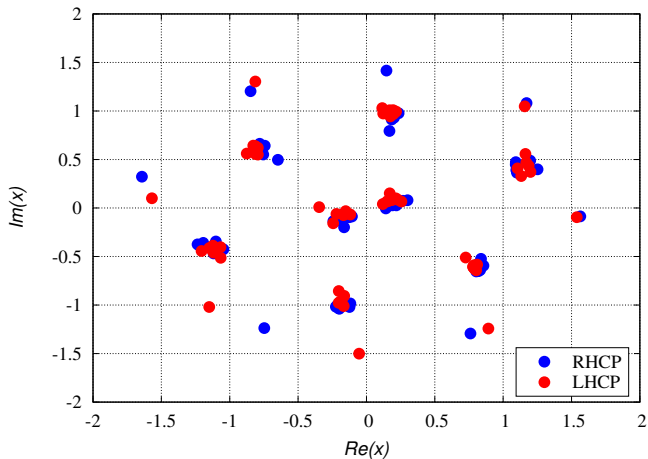


Fig. 3. 2D projections of the optimized 4D 64-ary constellation.

of the resulting optimized 4D constellation are reported in [17] and its 2D projected constellations are shown in Fig. 3. In the following, we denote this 4D constellation by 64-OPT. As it can be observed in Fig. 3, the 2D projected symbols onto the two polarizations are correlated. Indeed, most of the 64 4D symbols have a 2D projection in one of the eight clouds at the center of the constellation, whereas some of them have an isolated 2D projection. This implies that it is possible to correctly detect the original 4D symbol when an isolated 2D symbol is correctly detected on one polarization, even if the corresponding 2D symbol on the other polarization is completely corrupted by the channel. This peculiarity of the 4D design, which is not present in the Cartesian-based designs, improves the robustness of the system against the fading. However, this does not hold any longer if the correctly detected 2D symbol belongs to one of the eight clouds: in this case, the information conveyed by the other polarization is necessary to correctly identify the original 4D symbol. This is the main reason why a simpler detector operating separately on the two polarizations (i.e., treating the received samples from different polarizations as independent) would have a poorer performance than the optimal detector even when the channel does not introduce any cross-polar correlation. A performance comparison over the AWGN channel among these optimized 4D constellations with respect to other 4D constellations from the literature is also presented in [17], where significant gains are shown.

#### IV. NUMERICAL RESULTS

In this section, we first evaluate the PAMI for the chosen constellations, and then validate their performance over all the considered channels in terms of bit error rate (BER). The assumed abstract scenario is the downlink of a typical mobile satellite service.

##### A. PAMI Comparison

A Monte Carlo approach has been adopted in order to get reliable estimates of the expectation in (3). More precisely,  $3 \times 10^5$  channel realizations have been simulated. For the Rice and LMS channels, a XPD equal to 23 dB has been assumed,

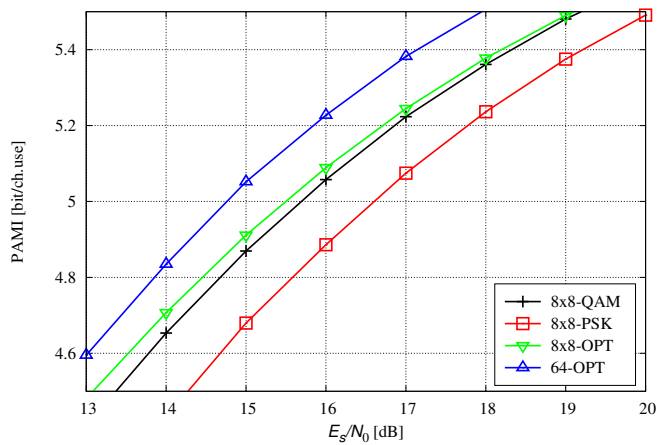


Fig. 4. PAMI over Rayleigh fading channel.

which is a value typical for professional equipment, and has been included in the channel realizations as in [21]. Moreover, the polarization correlation coefficients that characterize the small-scale fading have been assumed equal to 1 (for the transmit antennas) and 0.2 (for the receive antennas), as in [5]. Since we are interested in assessing the performance in the worst case scenario, for the LMS channel only the BAD state has been considered [20]. Therefore, the triplet of parameters required by the Loo distribution of the LMS model has been set to values typical for a urban environment with heavy shadowing, namely  $(\alpha, \psi, MP) = (-8.2585, 3.1711, -12.8542)$  dB, where  $\alpha$  and  $\psi$  are respectively the mean and the standard deviation of the lognormal distribution, and  $MP$  is the average power of the Rayleigh component. A time interleaver is typically used in LMS channels to render the channel relatively fast fading. However, we do not consider a time interleaver towards understanding the robustness of the proposed scheme. Moreover, the Doppler effect caused by the mobility has been included by considering a carrier frequency equal to 2.2 GHz and a mobile speed of 50 km/h as in [5].

For a PAMI around 5 bits/ch.use, 64-OPT shows a gain around 0.8 dB over 8x8-OPT over the Rayleigh channel, as shown in Fig. 4. This gain increases to 1 dB over 8x8-QAM, and even more over 8x8-PSK. It is worth noting that over the AWGN channel with the same PAMI, the gain provided by 64-OPT over 8x8-OPT is not exceeding 0.2 dB, as shown in [17]. Such a result confirms that the correlation over the polarization enhances the reliability of the system.

Over the Rice channel, the gains provided by 64-OPT progressively reduce: down to 0.4 dB over 8x8-OPT, and 0.7 dB over 8x8-QAM (at a PAMI around 5 bits/ch. use). This is caused by the relative reduction in the power of the multipath component (i.e., for increasing values of the  $K$ -factor of the Ricean distribution). This behavior is shown in Fig. 5 and Fig. 6. In Fig. 7, it can be seen that the shadowing further reduces the gains provided by the 4D optimization: only 0.2 dB over 8x8-OPT, and 0.4 dB over 8x8-QAM.

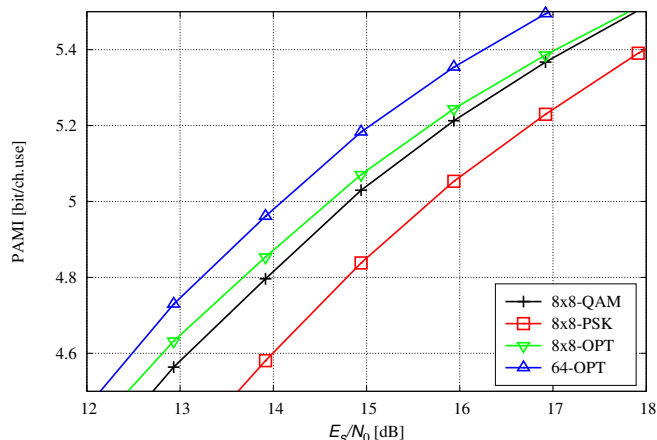


Fig. 5. PAMI over Rice fading channel with  $K = 0$  dB.

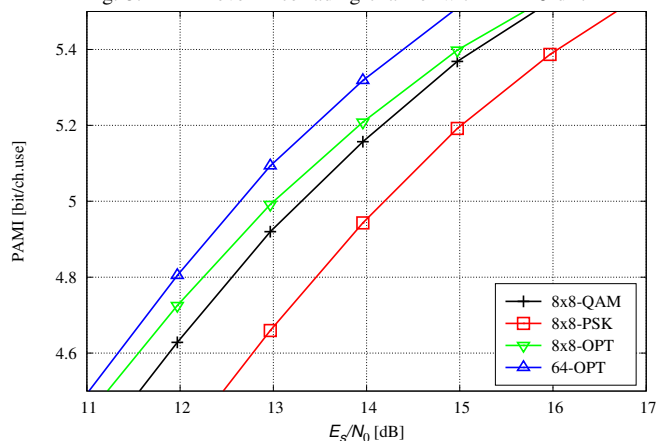


Fig. 6. PAMI over Rice fading channel with  $K = 5$  dB.

### B. BER Evaluation

In order to validate the results provided by the PAMI, we use a LDPC code with rate  $R = 5/6$  and code length  $n = 64800$  bits in all scenarios. As predicted by the PAMI computations, the 64-OPT constellation is more robust against the fading than all the other constellations. Moreover, the gains obtained in terms of PAMI (and shown in Figs. 4-7) relative to 64-OPT over the other constellations can be seen in the BER curves as well, as reported in Figs. 8-11.

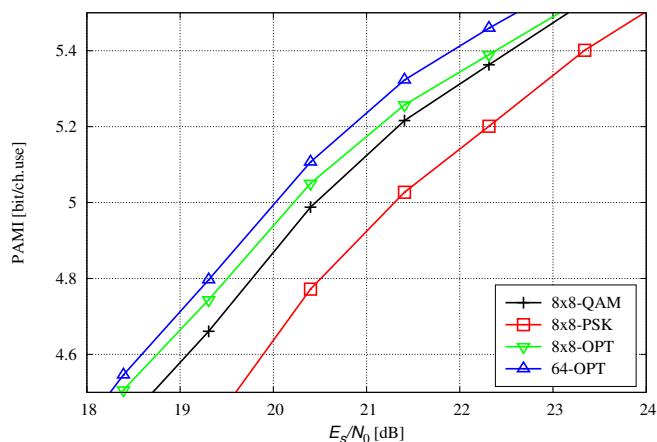


Fig. 7. PAMI over LMS channel.

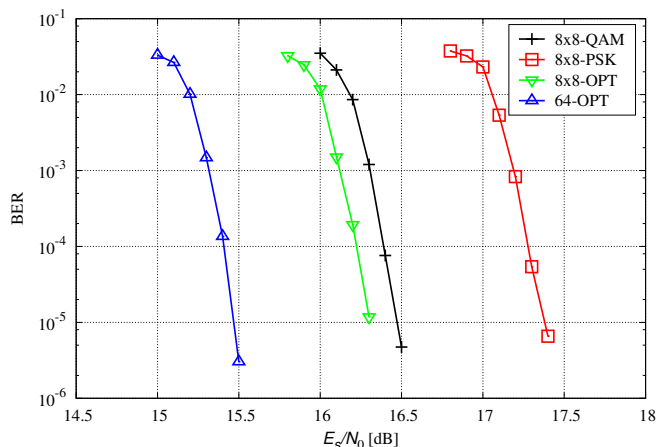


Fig. 8. BER curves over the Rayleigh channel.

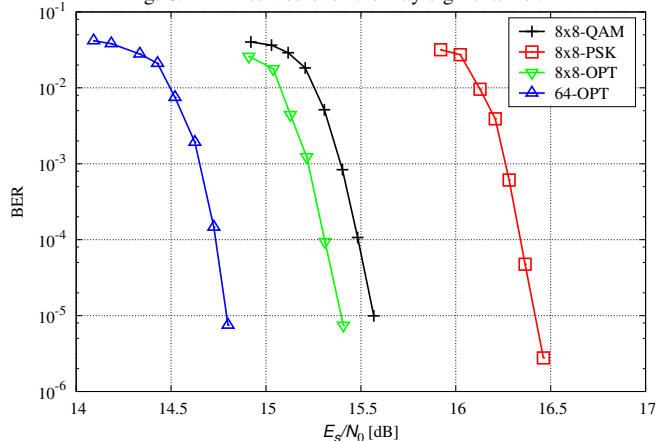


Fig. 9. BER curves over the Rice channel with  $K = 0$  dB.

### C. Relations to Dual-Polar MIMO

Exploiting dual polarizations to incorporate the MIMO paradigm has been studied in a number of works including [3]-[5]. Spatial multiplexing has been seen as a predominant candidate for satellite-only S-band applications [4]. The use of the Cartesian product of 2D constellations on the two polarizations coupled with joint detection of the two streams leads to the traditional MIMO paradigm with well known constellations. Further, the use of 8x8-OPT would still be

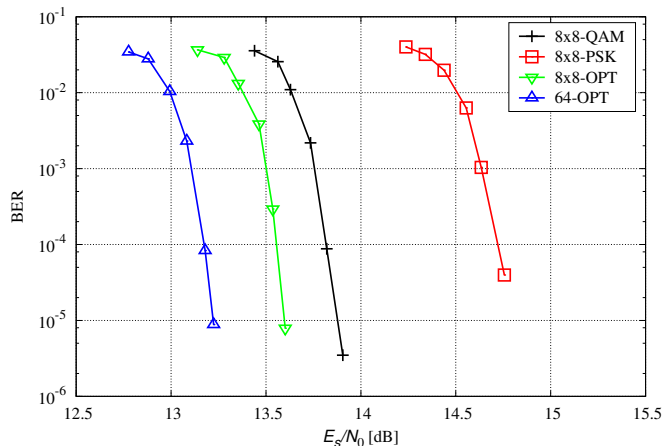


Fig. 10. BER curves over the Rice channel with  $K = 5$  dB.



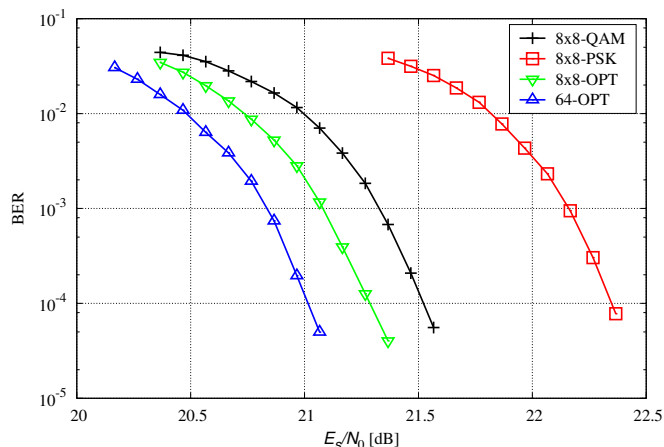


Fig. 11. BER curves over the LMS channel.

a dual-polar MIMO spatial multiplexing system. However, the constellation is chosen differently in this case, and this provides additional gains over spatial multiplexing. Finally, the use of 64-OPT can be construed as a polarization code which exploits the two polarizations to yield SNR gain (coding gain) by improving the robustness of the system against the fading. It would be interesting to extend the constellation design in the temporal dimension for use in conjunction with STC like the Golden code [5]. This is left for future work.

## V. CONCLUSIONS

In this paper, we have compared the performance of a 64-ary optimized 4D constellation with independent transmissions of two 2D constellations on the two polarizations. Three channel models have been considered: the Rayleigh flat fading channel, the Rice fading channel, and the LMS channel. Our results indicate that the optimized constellation in 4D outperforms all the Cartesian-based constellations. This also indicates that the 4D optimization provides a higher robustness against the fading, stemming from the additional correlation introduced between the polarizations. An even better performance is expected if the fading statistics and other channel characteristics (such as the polarization correlation and the mobility effects) were considered during the constellation design. Therefore, future investigations will be focused on an environment-dependent constellation design taking into account the partial CSI available at the transmitter. Finally, by casting the contribution in the dual-polar MIMO framework, the paper indicates the importance of constellation design while opening up new avenues for joint constellation-polarization-time designs.

## REFERENCES

- [1] V. Tarokh, N. Seshadri, and A. R. Calderbank, "Space-time codes for high data rate wireless communication: Performance criterion and code construction," *IEEE Trans. Inform. Theory*, vol. 44, no. 2, pp. 744–765, Mar. 1998.
- [2] T. Marzetta, "Noncooperative cellular wireless with unlimited numbers of base station antennas," *IEEE Trans. Wireless Commun.*, vol. 9, no. 11, pp. 3590–3600, 2010.
- [3] P. Arapoglou, K. Liolis, M. Bertinelli, A. Panagopoulos, P. Cottis, and R. De Gaudenzi, "MIMO over satellite: A review," *IEEE Communications Surveys Tutorials*, vol. 13, no. 1, pp. 27–51, 2011.

- [4] J. Kyröläinen, A. Hukkonen, J. Ylitalo, A. Byman, B. Shankar, P.-D. Arapoglou, and J. Grotz, "Applicability of MIMO to satellite communications," *International Journal of Satellite Communications and Networking*, vol. 32, no. 4, pp. 343–357, 2014.
- [5] B. Shankar, P. Arapoglou, and B. Ottersten, "Space-frequency coding for dual polarized hybrid mobile satellite systems," *IEEE Trans. Wireless Commun.*, vol. 11, no. 8, pp. 2806–2814, Aug 2012.
- [6] S. G. Srinivasan and M. Varanasi, "Constellation design for the noncoherent MIMO rayleigh-fading channel at general SNR," *IEEE Trans. Inform. Theory*, vol. 53, no. 4, pp. 1572–1584, April 2007.
- [7] S. Srinivasan and M. Varanasi, "Optimal constellations for the low-SNR noncoherent MIMO block rayleigh-fading channel," *IEEE Trans. Inform. Theory*, vol. 55, no. 2, pp. 776–796, Feb 2009.
- [8] D. Agrawal, T. Richardson, and R. Urbanke, "Multiple-antenna signal constellations for fading channels," *IEEE Trans. Inform. Theory*, vol. 47, no. 6, pp. 2618–2626, Sep 2001.
- [9] J. Giese and M. Skoglund, "Space-time constellation design for partial CSI at the receiver," *IEEE Trans. Inform. Theory*, vol. 53, no. 8, pp. 2715–2731, Aug 2007.
- [10] A. Yadav, M. Juntti, and J. Lilleberg, "Partially coherent constellation design and bit-mapping with coding for correlated fading channels," *IEEE Trans. Commun.*, vol. 61, no. 10, pp. 4243–4255, Oct 2013.
- [11] J. Giese and M. Skoglund, "Single- and multiple-antenna constellations for communication over unknown frequency-selective fading channels," *IEEE Trans. Inform. Theory*, vol. 53, no. 4, pp. 1584–1594, April 2007.
- [12] Y. Wu, V. Lau, and M. Patzold, "Constellation design for trellis-coded unitary space-time modulation," *IEEE Trans. Commun.*, vol. 54, no. 10, pp. 1896–1896, Oct 2006.
- [13] J. Boutros and E. Viterbo, "Signal space diversity: a power- and bandwidth-efficient diversity technique for the rayleigh fading channel," *IEEE Trans. Inform. Theory*, vol. 44, no. 4, pp. 1453–1467, Jul 1998.
- [14] G. Han, "Generalized PSK in space-time coding," *IEEE Trans. Commun.*, vol. 53, no. 5, pp. 790–801, May 2005.
- [15] G. Forney Jr. and L.-F. Wei, "Multidimensional constellations. i. introduction, figures of merit, and generalized cross constellations," *IEEE J. Select. Areas Commun.*, vol. 7, no. 6, pp. 877–892, Aug 1989.
- [16] A. K. Khandani and P. Kabal, "Shaping multidimensional signal spaces-part i: Optimum shaping, shell mapping," *IEEE Trans. Inform. Theory*, vol. 39, no. 6, pp. 1799–1808, Nov. 1993.
- [17] F. Kayhan, N. Mazzali, and B. Shankar M. R., "Constellation design in four dimensions under average power constraint," in *22nd IEEE Symp. on Comm. and Vehicular Tech. in the Benelux (SCVT)*, Nov. 2015, available at [http://www.eni.lu/snt/people/farbod\\_kayhan](http://www.eni.lu/snt/people/farbod_kayhan).
- [18] F. Kayhan and G. Montorsi, "Constellation design for memoryless phase noise channels," *IEEE Trans. on Wireless Commun.*, vol. 13, no. 5, pp. 2874–2883, May 2014.
- [19] M. Yofune, J. Webber, K. Yano, H. Ban, and K. Kobayashi, "Optimization of signal design for poly-polarization multiplexing in satellite communications," *IEEE Commun. Letters*, vol. 17, pp. 2017–2020, Nov. 2013.
- [20] R. Prieto-Cerdeira, F. Perez-Fontan, P. Burzigotti, A. Bolea-Alamañac, and I. Sanchez-Lago, "Versatile two-state land mobile satellite channel model with first application to DVB-SH analysis," *International Journal of Satellite Communications and Networking*, vol. 28, no. 5-6, pp. 291–315, 2010.
- [21] K. Liolis, J. Gómez-Vilardebó, E. Casini, and A. Pérez-Neira, "Statistical modeling of dual-polarized MIMO land mobile satellite channels," *IEEE Trans. Commun.*, vol. 58, no. 11, pp. 3077–3083, Nov 2010.
- [22] E. Kubista, F. Fontan, M. Castro, S. Buonomo, B. Arbesser-Rastburg, and J. Baptista, "Ka-band propagation measurements and statistics for land mobile satellite applications," *IEEE Trans. Veh. Tech.*, vol. 49, no. 3, pp. 973–983, May 2000.
- [23] W. Li, C. Law, V. Dubey, and J. Ong, "Ka-band land mobile satellite channel model incorporating weather effects," *IEEE Commun. Letters*, vol. 5, no. 5, pp. 194–196, May 2001.
- [24] J. Proakis and M. Salehi, *Digital Communications*, 5th ed., McGraw-Hill, Ed., 2008.
- [25] C. Loo, "A statistical model for a land mobile satellite link," *IEEE Trans. Veh. Tech.*, vol. 34, no. 3, pp. 122–127, Aug 1985.
- [26] G. Caire, G. Taricco, and E. Biglieri, "Bit-interleaved coded modulation," *IEEE Trans. Inform. Theory*, vol. 44, no. 3, pp. 927–946, May 1999.